

Electron-energy-loss spectroscopy of carbon nanometer-size tubes

P. M. Ajayan, S. Iijima, and T. Ichihashi

NEC Corporation, Fundamental Research Laboratory, 34 Miyukigaoka, Tsukuba, Ibaraki 305, Japan

(Received 2 November 1992)

Electron-energy-loss spectra from individual carbon nanometer-size tubes are presented. The bulk plasmon-loss ($\sigma + \pi$) peak seen at ~ 27 eV in graphite undergoes systematic shift towards lower energy, as the tube size is reduced. The low-energy-loss plasmon (~ 7 eV) due to the π electrons is weak and not well defined for very small tubes. It is seen that the peak shift depends on the number of layers that constitute the tubes and the tube diameter. The carbon K edge from nanometer-size tubes shows similar energy-loss features as in graphite. Thin amorphouslike glassy structures formed in the carbon soot also show shifts of peaks compared to graphite and graphitelike glassy structures. We conclude that the π electrons tend to behave less delocalized in small tubes, due to the curvature-induced strain, and contribute less to the collective excitations in structures with poorly developed c -plane ordering.

The discovery¹ and the large-scale synthesis² of carbon nanometer-size tubes have provided a big boost to research in the areas of carbon fiber growth³⁻⁵ as well as in the production and characterization of fullerene-related materials.⁶ Many authors have already speculated on this material's potential in practical applications.^{7,8} The unique structure of the tubes¹ has also provided a venue for theoreticians to speculate possible electronic structure and the corresponding implications.^{9,10} We present in this paper, electron-energy-loss spectra (EELS) from individual carbon tubules that show the change in the characteristic energy-loss peaks as a function of tube size. The results could prove to be a further step towards better understanding the electron interactions in carbon nanometer-size tube structures, which are essentially one-dimensional, highly oriented, and highly strained graphite, arranged helically in a cylindrical lattice with hollow inside.¹

The samples used in the study were prepared as discussed previously,² sonicated in ethanol, and a drop of the solution placed on a holey carbon grid used in electron microscopy. We used a Gatan parallel electron-energy-loss spectrometer connected to a TOPCON 002B transmission electron microscope operating at 200 kV. The energy resolution of the spectrometer is ~ 2 eV with a collection angle of ~ 10 mrad. The spectra were taken from individual tubes sticking out into the holes of the support grid by placing electron probes ~ 8 – 25 nm in size, corresponding to electron fluxes of approximately 250 – 100 A/cm², and the images of the corresponding tubes were recorded at high magnification after the spectra were collected. The observations were carried out at a fast pace (about a minute for spectra acquisition) so that electron-beam-induced degradation of the tubes into amorphous structure is minimized during the collection of the EELS spectra.

The collective excitations of the valence electrons (bulk plasmon) in graphite show two prominent characteristic energy-loss peaks,¹¹⁻¹³ one at about 7 eV, corresponding to the π orbitals which consist of one valence electron per carbon atom forming the $2p_z$ orbital perpendicular to the

graphite layers. The other three electrons form the strong interlayer planer σ bonds and the collective excitations of these and the single π electron give energy loss at ~ 27 eV. The free-electron theory predicts energy-loss peaks at ~ 12 and ~ 22 eV for the π and $\sigma + \pi$ bands, respectively, but the screening effects of the σ electrons in graphite force the two energy-loss peaks apart, to occur at the experimentally observed values of 7 and 27 eV.^{13,14} In amorphous carbon, the π peak is absent due to the lack of long-range ordering and only one peak occurs at ~ 25 eV.

The EELS from representative individual carbon nanometer-size tubes is presented in Figs. 1(a)–1(e) together with that from graphite for comparison. The images of the tubes corresponding to the spectra in Figs.

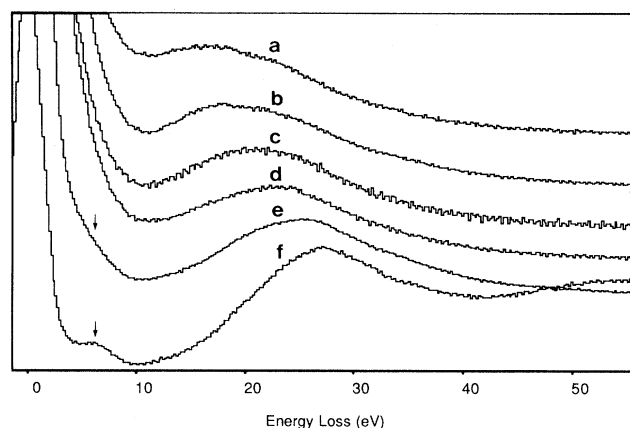


FIG. 1. EELS spectra from five different carbon nanometer-size tubes (a)–(e) and graphite (f). The spectra correspond to carbon nanometer-size tubes, the images of which are shown in Figs. 2(a)–2(e), respectively. Notice the gradual shift in the energy-loss peak seen at ~ 27 eV in graphite (f) towards lower energy. The arrows indicate the position of the π -electron energy-loss peak in graphite (f) and the large tube (e). In the smaller tubes (a)–(d), the peak is indistinguishable from the background. The spectra have been rescaled for displaying in one figure. The y axis has arbitrary units.

1(a)–1(e) are shown in Figs. 2(a)–2(e), respectively. There are two parameters that determine the size of the tubes: the number of layers that make up a tube and the diameter of the tube. The tubes shown in Figs. 2(a) and 2(b) have five and four layers each but the one in Fig. 2(a) has much smaller diameter since the inside hollow is small. The largest tube [Fig. 2(e)] has approximately 40 layers (note that the spacing between the layers is similar to the interplanar spacing in a graphite crystal which is 0.34 nm). From the spectra it is clear that with a decrease in the tube size, there is a systematic shift of the ($\sigma + \pi$) plasmon peak towards lower energy. The shift is substantial for small tubes, as much as ~ 9 eV for the smallest [Fig. 2(a)], when compared to the energy-loss peak in graphite [Fig. 1(f)]. The shift for the tube in Fig. 2(b) is similar to that in Fig. 2(a) although the diameter of the former is larger. One reason for this could be that in the former the number of layers is smaller although the diameter is large. It should be noted that the beam size is larger than the diameter of the tube in Fig. 2(a) and hence the unscattered portion of the beam will add intensity to the elastic peak in Fig. 1(a). However, the peak shift is much larger for the tube in Fig. 2(b) compared to the tube in Fig. 2(d) although the diameters are similar. This shows that there could be two parameters, the diameter of the tube as well as the number of layers constituting the tube, that affect the energy-loss spectrum. The shift of the $\sigma + \pi$ peak in large carbon nanometer-size tubes has been reported elsewhere,¹⁵ but this is the first time, to our knowledge, a systematic study is presented as a function of tube size (number of layers and diameter). The energy-loss peaks from the tubes are also seen to be broader compared to the one from graphite and this could be due to the orientation-related energy-loss dispersion in graphite as a range of orientations is probed by the transmitted electron beam in the cylindrical carbon lattice. This phenomenon of energy dispersion in graphite tubes (large) is seen when the probe is placed first at the center of the tube and then displaced towards the edges; the higher-energy plasmon peak shows a small shift downward in energy since the excitations corre-

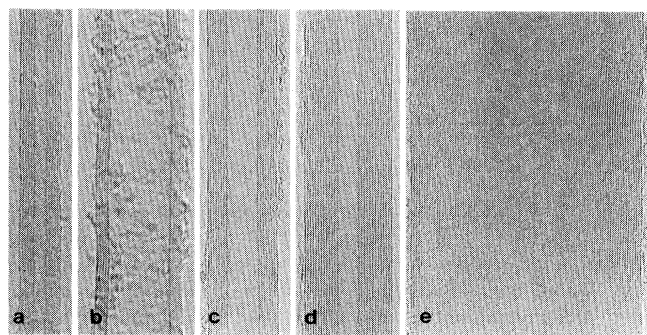


FIG. 2. High-resolution electron microscopy images from individual carbon nanotubes (a)–(e) from which EELS spectra were taken and presented in Figs. 1(a)–1(e). The spacing between layers in the images is ~ 0.34 nm. The tubes in (a) and (b) have almost the same number of layers (five and four, respectively) but the one in (b) is large due to the large inside hollow.

sponding to the scattering vector (incident beam) parallel to the c axis predominate as the beam scans preferentially the (002) basal planes of graphite that satisfy the Bragg condition. The effects of grazing incidence scattering at interfaces, such as for the smallest tube in Fig. 2(a) [spectrum Fig. 1(a)], may produce apparent shifts in plasmon peaks.¹⁶ But the effects of such aloof beams should be negligible, or similar, in the spectra for larger [Figs. 2(b)–2(e)] tubes. Moreover we are showing a systematic shift of the peaks as tube size is reduced. The effect of surface plasmons on the bulk plasmon peak shift will be small compared to what we have observed. The intensity of surface plasmons for such high-energy incident electrons and normal incidence would be almost negligible. In most cases the surface plasmon peak would occur at much lower energy which should be lower than the bulk plasmon peak for the smallest tube observed.

The plasmon energy-loss peak for the π electrons is not clearly seen for the smaller tubes (the ratio of the intensity of the π peak to the $\sigma + \pi$ peak decreases for smaller tubes) that we have studied [Figs. 1(a)–1(d)], compared with the well-defined peak of graphite [Fig. 1(f)]. For the largest tube [Fig. 1(e)] a small peak is seen around 6.8 eV, although this is not very clear in the figure (because of re-scaling the spectra to display all in one figure; see the arrow denoting the position of the peak). We also observed the spectra at primary electron energy of 120 kV, and the peaks due to the π electrons are seen as weak shoulders between 6–7 eV for smaller tubes. For very small tubes, having up to 10 layers, however, this peak is indistinguishable. We have looked at spectra from many small-sized tubes but have not been able to properly resolve this π -electron plasmon peak. It also appears that with the decrease in the size of the tubes the intensity of the π -electron plasmon excitation becomes weak.

Figure 3 shows plasmon loss peaks [Figs. 3(a) and 3(b)] from two different structures that are commonly observed in the raw soot produced during carbon arc discharge [images are shown in Figs. 3(c) and 3(d)]. The structures form complicated glassy knotted-graphitic carbon but they can be generally distinguished. One type has extremely thin graphitic structures (amorphouslike) mostly composed of single- or double-layered disordered c planes of graphite [Fig. 3(c)]. The second thicker structure [Fig. 3(d); graphitelike] consists of multilayered planes of twisted graphitic carbon [with better local ordering of the c planes in graphite in comparison to the structure in Fig. 3(c)]. The EELS from the structures show shifts in the positions of the $\sigma + \pi$ peak towards lower energy, in comparison to graphite but the shift for the former [Fig. 3(c)] is larger compared to the latter [Fig. 3(d)]. The π peak is visible in both but is weaker (compared with the $\sigma + \pi$ peaks) for the thinner structure. It seems that with a decrease in the amount of ordering of the c planes the contribution of the π electrons to the plasmon excitations decreases, as evidenced by the decrease in the π -loss peak intensity and the relative shift in the $\sigma + \pi$ peak towards lower energy. Another interesting observation in this regard is that for the tubular carbon structures consisting of only two or three layers (such structures are seen often as inside terminations in a

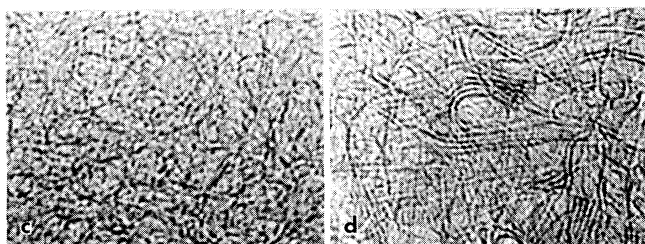
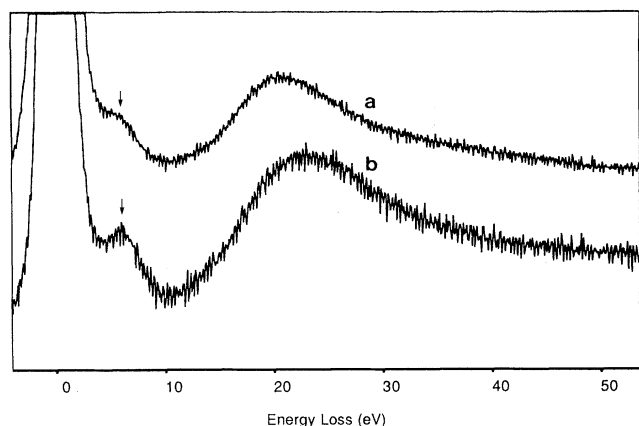


FIG. 3. EELS (a) and (b) corresponding to glassy graphitic structures shown in (c), which is amorphouslike, and (d), which is graphitelike. The peaks due to the π electrons occur at ~ 6.5 eV as shown by arrows. The y axis in spectra has arbitrary units.

tube), the interplanar spacing expands by up to 15% perhaps due to weakening of the van der Waals interplanar interaction.¹⁷

Figure 4 shows the K -edge excitations from the tubes [Fig. 4 (a)] from a medium-sized tube (~ 12 layers, ~ 10 nm) and Fig. 4(b) from a large tube (~ 25 layers, ~ 20 nm) and graphitic region [4(c)]. The spectra from the tubes look almost similar to that of graphite. All the spectra exhibit the peak at ~ 285 eV corresponding to the $1s$ to π transition and a broadened peak between 290 and 305 eV that corresponds to the K transitions to the σ orbitals. The fine structure present in these peaks is difficult to compare due to the limiting energy resolution but the peak at 292 eV seen in 4(b) and 4(c) is shifted by a small amount in the smaller tube 4(a) towards higher energy. The structure of the spectrum shown in 4(b), however, looks more like the K edge of graphite compared to 4(c) probably because the graphite region [spectrum 4(c)] was contaminated by amorphous carbon. Another small difference is that for the smaller tube 4(a) the π peak is broader and appears almost like a shoulder, shifted again slightly towards higher energy (by ~ 0.5 eV). This seems to be similar to the case of the spectrum of C_{60} solid¹⁸ where two humps are seen in the K -shell π -electron energy loss, one at 285 eV (same as in graphite) and one at 288 eV (from a second resonance due to the cage-strained π electrons).

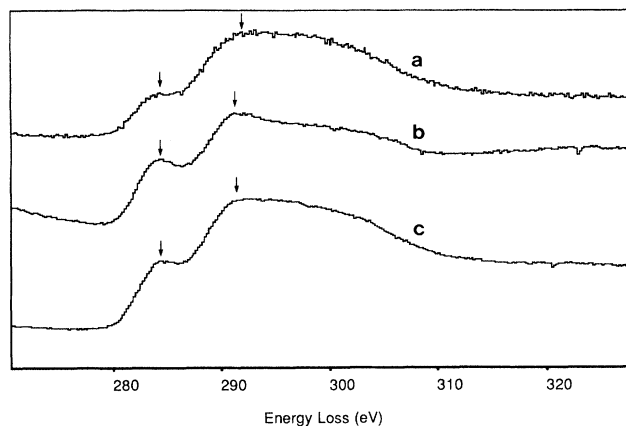


FIG. 4. EELS spectra for K -shell core electron excitations taken from tubes of two different sizes [medium size in (a) and large in (b)] and graphite. The positions of the peaks are almost coincident (arrows).

The systematic change in the position of the plasmon peak as a function of tube size suggests that the coupling between the π electron, and the σ electrons that bond the carbon atom to its three neighbors within a layer, changes with the number of layers that make the tube. Although the peak at ~ 7 eV is seen as due to the π resonance, it is a hybrid resonance that involves the cooperative effect of the π and σ electrons, and the position and strength of the peak (at ~ 7 eV) depend on the energy and strength of the onset of transitions that involve the σ electrons.¹² The systematic shift of the $\sigma + \pi$ peak (from 27 to < 20 eV) coincides with the decrease in the amplitude of the π resonance peak, as the tube sizes (or more precisely the number of layers) are reduced. The position of the $\sigma + \pi$ peak depends directly on the number of electrons that take part in the excitations (four valence electrons in graphite) and an effective decrease in the contribution from the π electron could shift this position to lower energies. The effective decrease in the screening effects could also force the peak towards the normal free-electron value of ~ 22 eV. In effect we are suggesting that the shift in the higher plasmon peak towards lower energy together with the weakening of the low-loss peak in small carbon nanometer-size tubes may be due to the weakening of the coupling between the π and σ electrons. The valence π electrons may be becoming less delocalized around the carbon atoms, effectively decreasing their contribution to collective plasma oscillations. One of the reasons for this localization could be due to the strain in the C-C bonds in the curled up graphite lattice, like the cage-strained π electrons in C_{60} .¹⁸

The coupling of plasmon excitation from the inner and outer surfaces of the tubes may also change the characteristics of the spectra and position of peaks but no quantitative treatment is available for any meaningful correlation of our data. A reason for the change in the energy-loss characteristics may be the lack of c -plane ordering in tubes that consist of very few layers. The structures that we presented in Fig. 3 with their respective spectra are pointers to this idea. It has been suggested that the pho-

non structure of a single infinite layer of graphite is quite different from bulk single-crystal graphite.¹⁹ The actual interaction of electrons between layers may be a function of the ordering of planes in that direction. This is also suggested by the change seen in the interplanar spacing as the number of layers are reduced.¹⁷ For tubes consisting of many layers, the graphitic character is restored due to better ordering between the planes. It has been reported before that the $\sigma + \pi$ peak shows shifts in energy in different carbon structures, depending on the density of the structures.²⁰ In our case the basic structure of carbon is the same (highly oriented graphite) in all the tubes but the density could be different due to the different size of the inside hollow. But the shift in the peaks, here, cannot be explained on the basis of density as the tube in Fig. 2(a) has a much smaller hollow compared to the one in Fig. 2(b) but shows a larger shift in the energy-loss peak compared to the latter. Moreover we have seen that the shifts in energy-loss peaks not only depend on the diameter of the tubes but also on the number of layers. The density of carriers might, however, change with this delicate interplay of the number of layers and the diameter. It has been predicted by theoreticians¹⁰ that at smaller sizes the tubes may behave as semiconductors or semimetals where the screening effects would be smaller com-

pared to graphite. It has also been reported that the carrier density decreases significantly with a decrease in the diameter of vapor-grown carbon fibers due to the dependence of the boundary scattering of carriers²¹ on the fiber diameter. Another parameter that determines the interplanar interactions could be the helicity in the carbon layers.¹ When interplanar interactions are absent (as in a single layer of graphite or as in a turbostatic structure with complete stacking disorder) graphite behaves as a zero-gap semiconductor and as the interactions between the layers (π -orbital overlap) develop, graphite behaves as a semimetal.²¹ In the case of the helical structure (with a certain amount of rotation of layers with respect to each other; not a perfect $ABAB \cdots$ -type stacking as in hexagonal graphite but almost like coincident lattice) the situation might be in between completely ordered and turbostatic. As the number of layers decreases, this effect, the kind of short-range stacking order, could become more pronounced. This would effectively decrease the strength of interaction between the layers and change the π -electron contribution to the plasmon loss. An interesting experiment is to look at the peak shifts in tubes that are helical and nonhelical.²² No such correlation has been found yet.

¹S. Iijima, *Nature* **354**, 56 (1991).

²T. W. Ebbesen and P. M. Ajayan, *Nature* **358**, 220 (1992).

³R. Bacon, *J. Appl. Phys.* **31**, 283 (1960).

⁴G. G. Tibbets, *J. Cryst. Growth* **66**, 632 (1984).

⁵J. S. Speck, M. Endo, and M. S. Dresselhaus, *J. Cryst. Growth* **94**, 834 (1989).

⁶D. Ugarte, *Nature* **359**, 707 (1992).

⁷P. Calvert, *Nature* **357**, 365 (1992).

⁸M. S. Dresselhaus, *Nature* **358**, 196 (1992).

⁹J. W. Mintmire, B. I. Dunlap, and C. T. White, *Phys. Rev. Lett.* **68**, 631 (1992).

¹⁰N. Hamada, S. Sawada, and A. Oshiyama, *Phys. Rev. Lett.* **68**, 1579 (1992).

¹¹Y. H. Ichikawa, *Phys. Rev.* **109**, B653 (1958).

¹²E. A. Taft and H. R. Philipp, *Phys. Rev.* **138**, A197 (1965).

¹³R. F. Egerton, *Electron Energy Loss Spectroscopy in the Elec-*

tron Microscope (Plenum, New York, 1986), Chap. 3.

¹⁴W. Y. Liang and S. L. Cundy, *Philos. Mag.* **19**, 1031 (1969).

¹⁵R. Kuzuo, M. Terauchi, and M. Tanaka, *Jpn. J. Appl. Phys.* **31**, L1484 (1992).

¹⁶P. M. Echenique, *Philos. Mag. B* **52**, L9 (1985).

¹⁷S. Iijima, *Chem. Scr.* **14**, 117 (1978–1979).

¹⁸H. Shinohara, H. Sato, and Y. Saito, *Jpn. J. Appl. Phys.* **30**, L1145 (1992).

¹⁹T. Aizawa, R. Souda, S. Otani, Y. Ishizawa, and C. Oshima, *Phys. Rev. Lett.* **64**, 768 (1990).

²⁰L. B. Leder and J. A. Suddeth, *J. Appl. Phys.* **31**, 1422 (1960).

²¹*Graphite Fibers and Filaments*, edited by M. S. Dresselhaus, G. Dresselhaus, K. Sugihara, I. L. Spain, and H. A. Goldberg (Springer-Verlag, Berlin, 1988), Chap. 8.

²²P. M. Ajayan, T. Ichihashi, and S. Iijima, *Chem. Phys. Lett.* **202**, 384 (1993).

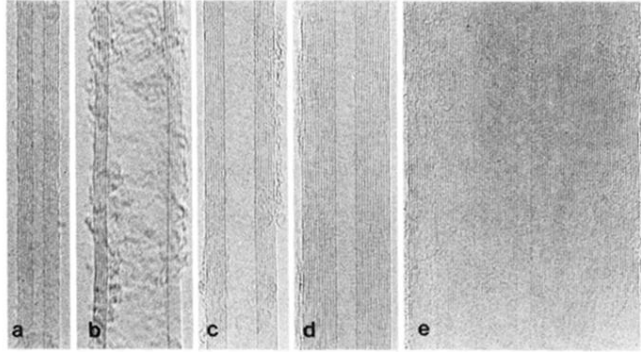


FIG. 2. High-resolution electron microscopy images from individual carbon nanotubes (a)–(e) from which EELS spectra were taken and presented in Figs. 1(a)–1(e). The spacing between layers in the images is ~ 0.34 nm. The tubes in (a) and (b) have almost the same number of layers (five and four, respectively) but the one in (b) is large due to the large inside hollow.

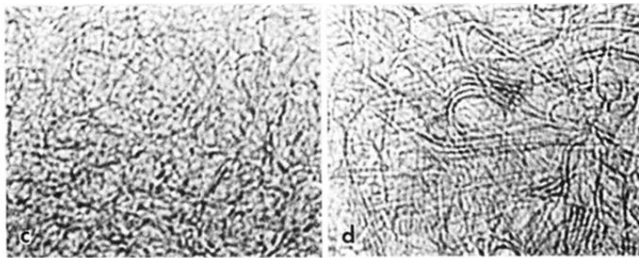
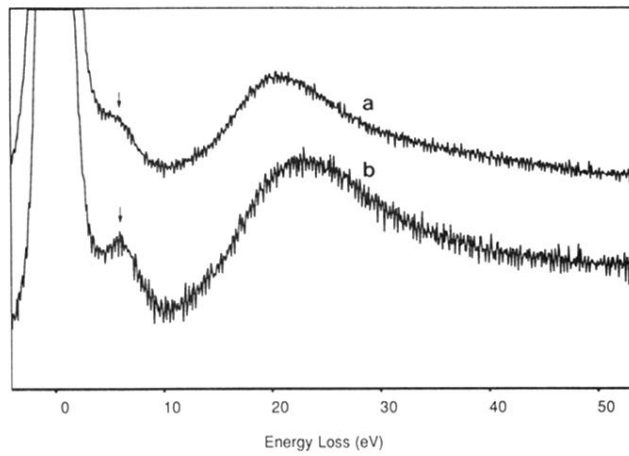


FIG. 3. EELS (a) and (b) corresponding to glassy graphitic structures shown in (c), which is amorphouslike, and (d), which is graphitelike. The peaks due to the π electrons occur at ~ 6.5 eV as shown by arrows. The y axis in spectra has arbitrary units.